



<b>Title</b>	Fabrication of Fe nanowires on yttrium-stabilized zirconia single crystal substrates by thermal CVD methods
<b>Author(s)</b>	Kawahito, A.; Yanase, T.; Endo, T.; Nagahama, T.; Shimada, T.
<b>Citation</b>	Journal of applied physics, 117(17), 17D506 <a href="https://doi.org/10.1063/1.4908150">https://doi.org/10.1063/1.4908150</a>
<b>Issue Date</b>	2015-05-08
<b>Doc URL</b>	<a href="http://hdl.handle.net/2115/59546">http://hdl.handle.net/2115/59546</a>
<b>Rights</b>	Copyright 2015 American Institute of Physics. This article may be downloaded for personal use only. Any other use requires prior permission of the author and the American Institute of Physics. The following article appeared in J. Appl. Phys. 117, 17D506 (2015) and may be found at <a href="http://doi.org/10.1063/1.4908150">http://doi.org/10.1063/1.4908150</a>
<b>Type</b>	article
<b>File Information</b>	Shimada.pdf



[Instructions for use](#)

## Fabrication of Fe nanowires on yttrium-stabilized zirconia single crystal substrates by thermal CVD methods

A. Kawahito, T. Yanase, T. Endo, T. Nagahama, and T. Shimada

Citation: *Journal of Applied Physics* **117**, 17D506 (2015); doi: 10.1063/1.4908150

View online: <http://dx.doi.org/10.1063/1.4908150>

View Table of Contents: <http://scitation.aip.org/content/aip/journal/jap/117/17?ver=pdfcov>

Published by the AIP Publishing

---

### Articles you may be interested in

[Templated fabrication and characterization of SiO<sub>2</sub> nanotube covered Fe nanowires](#)

*J. Appl. Phys.* **115**, 17B526 (2014); 10.1063/1.4868620

[Fabrication of single crystalline, uniaxial single domain Co nanowire arrays with high coercivity](#)

*J. Appl. Phys.* **115**, 113902 (2014); 10.1063/1.4868582

[Fabrication and magnetic properties of single-crystalline La<sub>0.33</sub>Pr<sub>0.34</sub>Ca<sub>0.33</sub>MnO<sub>3</sub>/MgO nanowires](#)

*Appl. Phys. Lett.* **103**, 113101 (2013); 10.1063/1.4819828

[Tuning the magnetization reversal process of FeCoCu nanowire arrays by thermal annealing](#)

*J. Appl. Phys.* **114**, 043908 (2013); 10.1063/1.4816479

[Self-catalysis: A contamination-free, substrate-free growth mechanism for single-crystal nanowire and nanotube growth by chemical vapor deposition](#)

*J. Chem. Phys.* **125**, 094705 (2006); 10.1063/1.2229195

---

Frustrated by old technology?      Is your AFM dead and can't be repaired?      Sick of bad customer support?

**It is time to upgrade your AFM**  
Minimum \$20,000 trade-in discount  
for purchases before August 31st

**Asylum Research is today's  
technology leader in AFM**

dropmyoldAFM@oxinst.com

**OXFORD**  
INSTRUMENTS  
*The Business of Science®*

# Fabrication of Fe nanowires on yttrium-stabilized zirconia single crystal substrates by thermal CVD methods

A. Kawahito,<sup>1</sup> T. Yanase,<sup>2</sup> T. Endo,<sup>3</sup> T. Nagahama,<sup>3</sup> and T. Shimada<sup>3,a)</sup>

<sup>1</sup>Graduate School of Chemical Science and Engineering, Hokkaido University, Kita-ku, Sapporo 060-8628, Japan

<sup>2</sup>Frontier Chemistry Center, Faculty of Engineering, Hokkaido University, Kita-ku, Sapporo 060-8628, Japan

<sup>3</sup>Faculty of Engineering, Hokkaido University, Kita-ku, Sapporo 060-8628, Japan

(Presented 4 November 2014; received 22 September 2014; accepted 23 October 2014; published online 23 February 2015)

Magnetic nanowires (NWs) are promising as material for use in spintronics and as the precursor of permanent magnets because they have unique properties due to their high aspect ratio. The growth of magnetic Fe whiskers was reported in the 1960s, but the diameter was not on a nanoscale level and the growth mechanism was not fully elucidated. In the present paper, we report the almost vertical growth of Fe NWs on a single crystal yttrium-stabilized zirconia ( $\text{Y}_{0.15}\text{Zr}_{0.85}\text{O}_2$ ) by a thermal CVD method. The NWs show a characteristic taper part on the bottom growing from a trigonal pyramidal nucleus. The taper angle and length can be controlled by changing the growth condition in two steps, which will lead to obtaining uniformly distributed thin Fe NWs for applications.

© 2015 AIP Publishing LLC. [<http://dx.doi.org/10.1063/1.4908150>]

## I. INTRODUCTION

Nanowires (NWs) have attracted attention because they have unique properties different from their bulk due to their high aspect ratio and diameter small enough for quantum confinement. The materials that can be fabricated as NWs include almost all materials, such as metallic NWs (Ni,<sup>1</sup> Au,<sup>2</sup> etc.) and semiconductor and insulating NWs (InGaAs,<sup>3</sup> Si,<sup>4</sup> ZnO,<sup>5</sup> etc.). Their characteristic physical properties and their applications have been determined, such as the anisotropic magnetoresistance of Ni,<sup>1</sup> plasmonics in Au,<sup>2</sup> quantum size effect in  $\text{In}_x\text{Ga}_{1-x}\text{As}$  transistors,<sup>3</sup> Si NW solar cells,<sup>4</sup> and ZnO chemical sensors.<sup>5</sup> Fe NWs in this study are expected to have an anisotropic magnetoresistance effect due to their large shape anisotropy. They are also expected for application in spintronic devices and the precursor of permanent magnets.

The template method<sup>6</sup> uses electroplating in an array of nanoholes produced by the anodic oxidization of aluminum. Although this method is straightforward and easy to operate, it has disadvantages such as difficult exfoliation from substrates, the crystallinity of the nanowires and relatively long reaction time. We used Chemical Vapor Deposition (CVD) for the growth of the Fe nanowires because the reaction is fast and useful as a method of fabricating NWs without using templates.

The CVD growth of Fe whiskers has been known since the 1960s.<sup>7</sup> However, the diameter of the whiskers was greater than  $1\ \mu\text{m}$  at that time. The factors controlling the diameter and the crystal orientation of the whisker had not been studied using modern nanotechnology. It is unknown whether or not the growth mode is the VS (vapor-solid) mechanism<sup>8,9</sup> or VLS (vapor-liquid-solid) mechanism.<sup>10</sup>

Modern nanowire growth techniques use catalytic nanoparticles, such as Au,<sup>11,12</sup> and we indeed observed a catalytic effect in the growth of the Fe NWs.<sup>13</sup> On the other hand, many reports have been found in the literature about nanowire formation without catalysts.<sup>14</sup>

In this paper, we report the fabrication of Fe NWs without catalysts by the thermal CVD method on the substrates of yttria-stabilized zirconia (YSZ). We also comment on how to control the shapes and growth mechanisms of the Fe NWs.

## II. EXPERIMENT

The reaction for the formation of the Fe NWs is considered as follows:

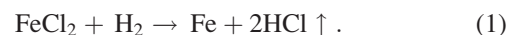


Figure 1 illustrates the equipment used in the present research. The furnace has three temperature-controllable zones which are labelled from upstream zone A, zone B, and zone C. A quartz tube (diameter of 43 mm) was placed in the furnace.  $\text{FeCl}_2 \cdot 4\text{H}_2\text{O}$  (purchased from Kanto Chemical Co., Inc.) was placed in zone B without any purification as the precursor. YSZ (110) substrates were installed in zone C after cleaning in an ultrasonic acetone bath.  $\text{FeCl}_2$  gas was

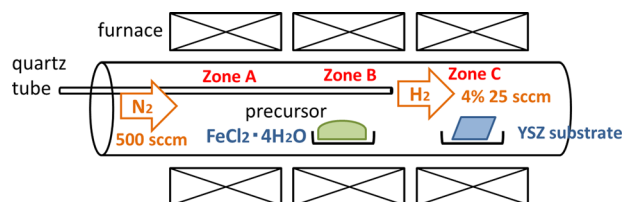


FIG. 1. Schematic drawing of the CVD equipment with the gas flow separation system used in the present study.

<sup>a)</sup>Author to whom correspondence should be addressed. Electronic mail: [shimadat@eng.hokudai.ac.jp](mailto:shimadat@eng.hokudai.ac.jp).

sublimated by a high temperature in zone B and carried to zone C by the flow of a carrier gas.  $\text{FeCl}_2$  was reduced by  $\text{H}_2$  according to Eq. (1) and the reduced Fe was grown as NWs on the substrates in zone C. The distance between the  $\text{FeCl}_2 \cdot 4\text{H}_2\text{O}$  and the substrates was approximately 8 cm.

$\text{FeCl}_2 \cdot 4\text{H}_2\text{O}$  in B zone was annealed at  $200^\circ\text{C}$  for 30 min to remove any crystal water prior to the CVD growth. The carrier gas (99.99%  $\text{N}_2$ ) was then flowed at the rate of 500 sccm. After removing the  $\text{H}_2\text{O}$  from the  $\text{FeCl}_2 \cdot 4\text{H}_2\text{O}$ , each zone of the furnace was heated to a preset temperature within 2–3 h. The temperatures of zone A and B were  $550^\circ\text{C}$  and  $600^\circ\text{C}$ , respectively. The temperature of zone C was from 800 to  $1000^\circ\text{C}$ , which will be denoted as the growth temperature of the Fe NWs. After the temperature of each zone reached its preset temperature, the reaction gas (3.9%  $\text{H}_2 + 96.1\%$  Ar) started to flow at the flow rate of 25 sccm which was maintained for 10–30 min, which is denoted as the growth time. The reaction gas was supplied through the inner 6-mm diameter quartz tube to zone C. This inner quartz tube separated the flow of reaction gas from that of the carrier gas before zone C. This separation prevents the reaction of  $\text{FeCl}_2$  with  $\text{H}_2$  before reaching the substrate.

After the reaction, the supply of the reaction gas and the heating was stopped and the system was cooled to room temperature by flow of the  $\text{N}_2$  carrier gas. We also adopted a two-step growth at different growth temperatures reported for the GaAs NW growth.<sup>15</sup> The temperature was kept high for a short time for the nucleation, and then, the temperature was stepwise decreased and kept at a certain temperature for the growth of the nuclei.

The morphology of Fe NWs was studied by Scanning Electron Microscopy (SEM; JEOL JSM-6500F and JSM-6390LVS). The crystal structure was examined by X-ray diffraction (XRD; Rigaku RINT2200). Magnetization of the sample was measured by a Vibrating Sample Magnetometer (VSM; Riken Denshi BHV-50) at room temperature.

### III. RESULTS AND DISCUSSION

Figure 2(a) shows an SEM image of the Fe NWs grown on the YSZ substrates. The NWs were obtained at  $850^\circ\text{C}$  for 30 min. From the SEM image of Fig. 2, it is observed that

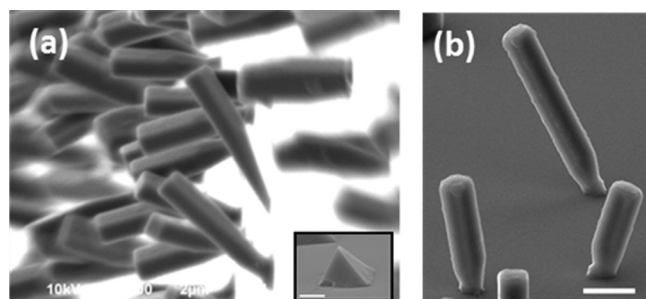


FIG. 2. SEM images of Fe NWs grown by one-step reaction at  $850^\circ\text{C}$  for 30 min. (a) and (b) were obtained by SEM and FE-SEM, respectively, at different magnifications. The base of the NWs has a characteristic shape. The inset of (a) shows the early stage of the growth (5 min) with a trigonal pyramidal nucleus which probably becomes the base of the NWs. The scale bar in (a) and its inset corresponds to  $5\ \mu\text{m}$ , while that in (b) corresponds to  $1\ \mu\text{m}$ .

the Fe NWs grew nearly vertically from the substrates and that they had a characteristic shape at the bottom, i.e., a tapered wall stemming from the base with a narrow neck. These Fe NWs had a diameter and length of approximately 0.3 and 6–10  $\mu\text{m}$ , respectively. The inset of Fig. 2(a), obtained by a short growth time (5 min), shows a trigonal pyramidal nucleus, which probably makes the base of the NWs have a characteristic shape. Figure 2(b) shows the FE-SEM image of the obtained Fe NWs with a high resolution. From this picture, the shape of the base is clearly observed, which resembles the nuclei shown in the Fig. 2(a) inset. It is also noted that the shape of the top of the NWs are square, suggesting that the growth orientation is [001].

The temperature range for the NW growth was determined to be  $850\text{--}900^\circ\text{C}$  for 10–30 min. Neither nucleation nor growth of the NWs was observed at a temperature higher than  $900^\circ\text{C}$ . On the other hand, when the reaction occurred below  $850^\circ\text{C}$ , nucleation was obtained but Fe was grown as a continuous film, not as NWs.

The Fe NWs in our experiments increased the diameter from the nuclei for a certain length, and then the side walls become parallel. This characteristic tapered shape at the bottom seems to be an important factor to determine the diameter of the NWs. The tapered shape has also been reported for Ge and ZnO, but the taper appears at the top.<sup>16,17</sup> There are few reports about the NWs with a taper at the bottom. The result of the two-step growth in the present experiment gives an important hint about the formation mechanism of the taper at the bottom.

Figure 3(a) shows the SEM image obtained by the two-step growth at  $850^\circ\text{C}$  for 10 min and  $800^\circ\text{C}$  for 30 min. The rate of the temperature change from a high temperature to a low one was  $-1.7^\circ\text{C}/\text{min}$ . The observed Fe NWs had bottom part and top part diameters of approximately 0.2 and 0.8  $\mu\text{m}$ , respectively, and the length of the taper part was 20–30  $\mu\text{m}$ , which was longer than the taper part in Fig. 2(a). Figure 3(b) shows a SEM image of the result of the growth at  $900^\circ\text{C}$  for 10 min and at  $850^\circ\text{C}$  for 30 min. The observed Fe NWs had bottom part and top part diameters of approximately 0.2 and 0.3  $\mu\text{m}$ , respectively, and the length of the taper part was 0.3  $\mu\text{m}$ , which was shorter than the taper part

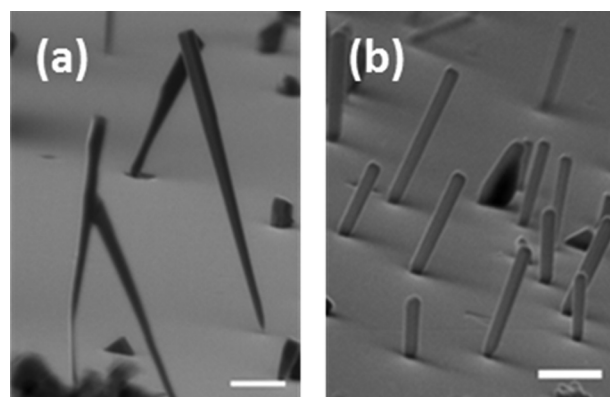


FIG. 3. SEM images of Fe NWs in the two-step growth at (a)  $850^\circ\text{C}$  (10 min) and  $800^\circ\text{C}$  (30 min). The scale bar indicates  $5\ \mu\text{m}$ . (b)  $900^\circ\text{C}$  (10 min) and  $850^\circ\text{C}$  (30 min). The scale bar indicates  $5\ \mu\text{m}$ . The rate of the temperature drop is  $-1.7^\circ\text{C}/\text{min}$  for both cases.



in Fig. 2(a). This result indicates that we can control the tapered shape of the NWs by adopting the two-step growth.

The factor determining the length and the angle of the taper seems to be attributed to the change in the growth speed of each plane of Fe at different temperatures. In the case of a low temperature, the growth rate in the vertical ([001]) direction is greater than that of the horizontal tapered planes, which results in Fe NWs with a larger taper part (Fig. 3(a)). On the other hand, at higher temperatures, the horizontal growth rate is greater than that of the vertical growth.

Figure 4 shows the result of the XRD measurement after the CVD at with the same conditions as that of Fig. 2(a). There were two main peaks corresponding to  $\alpha$ -Fe (bcc) 110 and 200. The other peaks are from the YSZ substrate. No peaks from compounds, such as  $\text{FeCl}_2$  and  $\text{Fe}_2\text{O}_3$ , were observed. This indicated that all of the  $\text{FeCl}_2$  precursor was reduced by  $\text{H}_2$  to the  $\alpha$ -Fe single crystal. Since the peak area of 200 at the higher diffraction angle is much larger than that of the 110 peak, the vertically grown Fe NWs are oriented to 001. This result is consistent with the square shape of the basal plane of the vertically grown NWs (Fig. 2(b)).

Which of VLS and VS mechanisms apply to our NWs is now discussed. In this study, the trigonal pyramidal nuclei were obtained, which means that these nuclei have the possibility to be self-catalysts for the VS mechanism. In the early stage of growth, although Fe grows both vertically and horizontally, their growth speed depends on the conditions of the temperature, resulting in the formation of the tapered shape. The shape of the taper is changed by the temperature. After the diameter of the Fe NW reached a certain value, the horizontal growth stops and  $\alpha$ -Fe (100) as the stable planes appeared as the side walls, and only then vertical growth continues. Precisely understanding the transition mechanism is important to control the diameter of the Fe NWs. In order to reduce the diameter of the Fe NWs, for example, the transition from the nucleation to NW growth must occur earlier, and the taper angle must be minimized, both of which will be achieved by optimizing the growth conditions.

Finally, we present the magnetic properties. Figure 5 shows the magnetization curve of the sample with the magnetic field parallel and perpendicular to the substrate surface. The substrate signals, which were almost linear, were

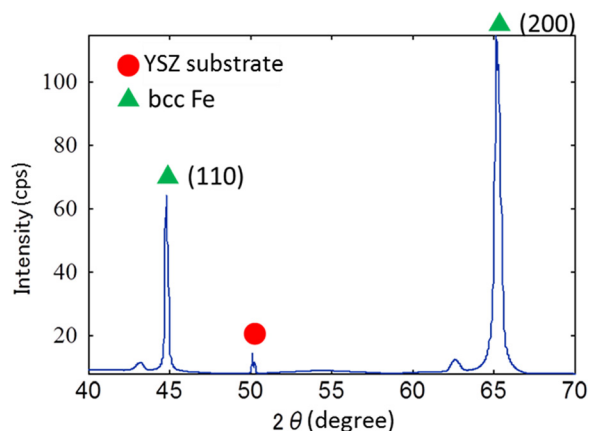


FIG. 4. Result of XRD measurement of vertically grown Fe NWs.

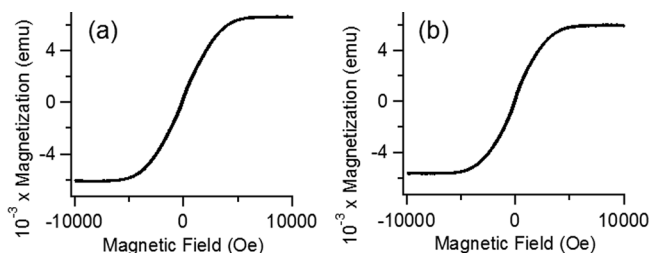


FIG. 5. Magnetization curves of Fe NWs. (a) Perpendicular to the sample surface and (b) parallel to the sample surface.

separately measured and subtracted from the sample data after normalization, assuming a saturation beyond 7000 Oe. The saturation magnetization was  $\sim 6 \times 10^{-3}$  emu. The sample size was measured to be  $1.7 \times 10^{-2} \text{ cm}^2$ . Using the saturation magnetization of bulk Fe ( $1.7 \times 10^3 \text{ emu cm}^{-3}$ ),<sup>18</sup> the averaged sample thickness was estimated to be  $6 \times 10^{-3} \times 1.7 \times 10^3 / 1.7 \times 10^{-2} = 2 \times 10^{-5} \text{ cm} = 200 \text{ nm}$ . It is consistent with the SEM images of the Fe NWs, roughly showing a length of  $2 \mu\text{m}$  and a coverage of 10%. The shapes of the curves with different magnetic field directions are similar, showing very little anisotropy. This does not agree with the shape of the NWs, but it might be due to multiple-alignment of the NWs, partial oxidization of the NWs, and existence of bulk Fe films at the periphery of the sample as an impurity.

#### IV. CONCLUSIONS

In this study, we fabricated Fe NWs by thermal CVD methods on YSZ (110) substrates. The path of reaction gas was separated from that of the carrier gas, which enabled the precise control of the supply of the flux of the raw material without any undesirable reaction. The top of the obtained Fe NWs was square showing Fe [001] growth orientation. There were taper shapes at the bottom, which stemmed from a trigonal pyramidal nucleus. We adopted a two-step growth method to accurately control their shape. As a result, the shape of the taper was dramatically changed by the temperature. The change in the taper shape seemed to be attributed to the difference in the horizontal and vertical growth rate of each plane of the Fe NWs depending on the growth temperature. Magnetization was qualitatively consistent with the amount of NWs.

#### ACKNOWLEDGMENTS

The present work was partly supported by CREST-JST. The authors would like to thank Professor S. Kikkawa (Hokkaido Univ.) and his laboratory members for kindly allowing the use of the VSM equipment and for their valuable discussions.

<sup>1</sup>K. T. Chan *et al.*, *Nano Lett.* **10**, 5070 (2010).

<sup>2</sup>S. S. Chang, C. W. Shih, C. D. Chen, W. C. Lai, and C. R. C. Wang, *Langmuir* **15**, 701–709 (1999).

<sup>3</sup>J. J. Gu *et al.*, *IEEE Electron Device Lett.* **33**(7), 967 (2012).

<sup>4</sup>L. Tsakalacos *et al.*, *Appl. Phys. Lett.* **91**, 233117 (2007).

<sup>5</sup>X. Liu *et al.*, *Sens. Actuators, B* **176**, 22 (2013).

<sup>6</sup>N. Martinho *et al.*, *Angew. Chem. Int. Ed.* **51**, 11995 (2012).

<sup>7</sup>S. Brenner *et al.*, *Acta Metall.* **4**, 62 (1956).

- <sup>8</sup>E. Comini *et al.*, *Prog. Mater. Sci.* **54**, 1 (2009).
- <sup>9</sup>Chunnian He *et al.*, *Mater. Chem. Phys.* **97**, 109 (2006).
- <sup>10</sup>R. S. Wagner *et al.*, *Appl. Phys. Lett.* **4**, 89 (1964).
- <sup>11</sup>W. Hwang *et al.*, *Chem. Mater.* **20**, 6041 (2008).
- <sup>12</sup>T. Ishida *et al.*, *Angew. Chem. Int. Ed.* **46**, 7154 (2007).
- <sup>13</sup>T. Yanase, A. Kawahito *et al.*, *RSC Adv.* **4**, 27620 (2014).
- <sup>14</sup>A. Fontcuberta *et al.*, *Appl. Phys. Lett.* **92**, 063112 (2008).
- <sup>15</sup>H. J. Joyce *et al.*, *Nano Lett.* **7**, 921 (2007).
- <sup>16</sup>P. Periwal *et al.*, *APL Mater.* **2**, 046105 (2014).
- <sup>17</sup>Y. H. Yang *et al.*, *Nano Lett.* **7**, 3879 (2007).
- <sup>18</sup>J. M. D. Coey, *Magnetism and Magnetic Materials* (Cambridge University Press, Cambridge, 2010).